# Image segmentation algorithm based on the second clustering and level set method

Hai Jie[1], Wu Li[1], Wu Haiyan[1], Du Hailong[1]

1 .School of Electronics and Information Engineering SIAS International University, Xin Zheng, Henan, 451150, China

**Key words:** level set; image segmentation; intelligent algorithm; cluster analysis

**Abstract.** Improve the level set algorithm by Lagrangian particle enhanced replanting algorithm and increase the reduced segmentation accuracy brought about by the algorithm for uneven image pixel for medical CT image. Based on Literature [4], the combination of Lagrangian particle enhanced replanting algorithm and level set algorithm is adopted, the convergence of velocity field for singular point is promoted through increase of velocity vector and unit normal vector and the medical CT image segmentation method of hybrid level set (LPRLS) based on Lagrangian particle enhanced replanting algorithm is proposed in the Thesis. Calculate the Lagrangian labeled particle before calculating the formula of horizontal set to rebuild the embedded interface in order to improve the mass conservation property of level set algorithm; improve the convergence of velocity field for singular point and topological change point through increasing velocity vector and unit normal vector in order to handle the singularity of interface and complicated geometric correlation. The simulation results of algorithm indicate that the performance of the proposed algorithm is greatly improved compared with the original algorithm. It can be concluded from the simulation results that the existing insufficiency is the proportion of error identification of the algorithm.

## Introduction

In recent years, Osher and Sethian, etc., the scholars in image processing direction jointly studied and proposed the segmentation algorithm for level set (LS) and the main idea was to map the low-dimensional closed two-dimension curve to the high-dimensional level set for processing with a view to strengthening the stability of image segmentation algorithm. Even so, the singularity and complicated geometric correlation of image interface play a significant influence on the level set algorithm; so the proper handling of the above problems is very important to improve the application effect of level set segmentation algorithm in medical imaging such as CT and X-ray and favorable to improving the performance of the algorithm in dealing with the problems such as poor contrast, uneven pixel and fuzzy boundary with image segmentation problems in medical imaging[2-3].

## Level set algorithm based on particle

The essence of level set algorithm is to turn the image segmentation problem to hyper curved surface activity in high-dimensional space as shown in Fig.1. The embedded interface $\Gamma \in \mathbb{R}^3$ can be defined as the signed distance function of zero level set, $\phi$. So the formula for iterative evolution algorithm of standard level set is as follows[11-12]:

$$\frac{\partial \phi}{\partial t} + \bar{V}, \nabla \phi = 0 \tag{1}$$

Where the velocity field $\bar{V}$ is generally given by the external flow method and the evolution equation is solved through the narrow area near the surface.

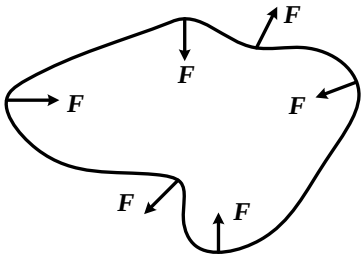


Fig.1 Schematic Diagram for Level Set Segmentation

Even when the contour continuously flows, the level set function can easily process the smooth contour. The reinitialization of level set can ensure the distance property of smooth signal, $|\nabla\phi|=1$. So it is required to solve through the following equation until the state become stable:

$$\phi_\tau + \mathrm{sgn}(\phi_0)(|\nabla\phi|-1)=0 \qquad (2)$$

Where $\tau$ is the pseudo time for reinitialization of level set equation, so the diffused sign function can be defined as:

$$S=\phi\Big/\sqrt{\phi^2+(1-|\nabla\phi|)^2\nabla x^2} \qquad (3)$$

Based on Godunov solution[3] and the monotonicity of function, the compulsory execution can be conducted for Formula (2) based on the following time limit steps:

$$\frac{\nabla\tau}{\nabla x}|S|\le\frac{1}{2} \qquad (4)$$

Then, the space and time derivatives for Formula (1) and Formula (2) can be calculated based on the narrow area of fifth-order WENO format[14] and third-order TVD-Runge-Kutta method[15] near the surface. The geometric quantity such as unit normal vector $\vec{n}$ and local curvature $k$ can be calculated as follows through level set formula:

$$\begin{cases}\vec{n}=\nabla\phi/|\nabla\phi| \\ k=\nabla\cdot\vec{n}=\nabla\cdot(\nabla\phi/|\nabla\phi|)\end{cases} \qquad (5)$$

**Level set method of hybrid particle**

For the method, Eulerian level set algorithm[16] and Lagrangian particle algorithm are combined and the Lagrangian massless particle is adopted to correct the level set function for area to be solved of image interface. Two groups of particles are randomly placed near the interface of narrow band and attract the interface to the correct side; the positive particle tends to the side of $\phi>0$ and recessive particle tends to the side of $\phi\le 0$; Lagrangian particle will produce convection at the given velocity:

$$\frac{d\vec{x}_p}{dt}=\vec{u}(\vec{x}_p) \qquad (6)$$

Where $\vec{x}_p$ is the particle position and $\vec{u}(\vec{x}_p)$ is the velocity vector of particle. Due to dissipation loss of the evolution equation, the flowing feature information is totally saved. Then, the third-order TVD Runge Kutta method is used to solve the evolution equation of time derivative.

There is a position and range radius for each particle to make up the position error caused by limitation of level set function. The radius of each particle is defined according to the maximum value and minimum value of grid. According to the maximum and minimum delimitation values for particle radius of Formula (6), calculate by the following equations:

$$\begin{cases}r_{\min}=a\cdot\min(\Delta x,\Delta y,\Delta z) \\ r_{\max}=b\cdot\min(\Delta x,\Delta y,\Delta z)\end{cases} \qquad (7)$$

In conclusion, the range radius of each particle can be defined as follows:

$$r_p = \begin{cases} r_{\max}, & if\ s_p\phi(\bar{x}_p) > r_{\max} \\ s_p\phi(\bar{x}_p), & if\ r_{\min} \le s_p\phi(\bar{x}_p) \le r_{\max} \\ r_{\min}, & if\ s_p\phi(\bar{x}_p) < r_{\min} \end{cases} \quad (8)$$

Where $s_p$ is used to indicate the positive and negative property of particle and the following equations can be used to define and describe:

$$s_p = \begin{cases} +1, & if\ \phi(\bar{x}_p) > 0 \\ -1, & if\ \phi(\bar{x}_p) < 0 \end{cases} \quad (9)$$

On the image surface easily to be solved with clear interface and even pixel, the solution for level set function is sufficiently accurate and the particle will not drift far away from the interface. However, in the area not easily to be solved with uneven pixel and fuzzy boundary, the calculation of level set function will cause mass loss and the particle will drift far away from the interface. The escaped positive (or negative) particle from the interface can define local level set function based on grid point, particle radius and particle sign. The correction of level set function set can be realized through comparison of level set function value of grid and the local level set function value of escaped particle. According to the sign for level set function of grid, the local level set function of the escaped positive and negative particles can be respectively defined as follows:

$$\phi_p(x) = \begin{cases} s_p\left(r_p - \left|x - x_p\right|\right), if\ \phi(x) \le 0 \\ s_p\left(r_p + \left|x - x_p\right|\right), if\ \phi(x) > 0 \end{cases} \quad (10)$$

$$\phi_p(x) = \begin{cases} s_p\left(r_p - \left|x - x_p\right|\right), if\ \phi(x) > 0 \\ s_p\left(r_p + \left|x - x_p\right|\right), if\ \phi(x) \le 0 \end{cases} \quad (11)$$

Through comparison of the areas for $\phi > 0$ and $\phi \le 0$ with the function values of $\phi^+$ and $\phi^-$ for level set of grid, the level set function can be rebuilt based on error correction method. The function values of $\phi^+$ and $\phi^-$ for level set are respectively located in positive area and negative area and then calculate the function value of defined local level set through escaped particles. Each corner for the areas of $\phi(x) > 0$ and $\phi(x) \le 0$ can be calculated through the following equations:

$$\begin{cases} \phi^+ = \max\left(\phi_p, \phi^+\right) \\ \phi^- = \max\left(\phi_p, \phi^-\right) \end{cases} \quad (12)$$

The function values of $\phi^+$ and $\phi^-$ for level set can be synthesized to the single level set function through setting the equivalent variable $\phi$ of $\phi^+$ and $\phi^-$. The level set is of the minimum value at each grid point. The variable $\phi$ can be defined as follows:

$$\phi = \begin{cases} \phi^+, & if\ \left|\phi^+\right| \le \left|\phi^-\right| \\ \phi^-, & if\ \left|\phi^+\right| > \left|\phi^-\right| \end{cases} \quad (13)$$

## Simulation experiment and analysis

Parameter of simulation equipment: the processor is i7 2.4GHz and the memory is 4G ddr1333. Selection of simulation platform: matlab2012a. Experimental subjects: the common medical CT images which are respectively angiography CT, tumor CT, breast CT, brain CT and chest CT. The evaluation indicators are the identification rate, operation time and variance of image segmentation algorithm.

Setting of simulation parameters: angle $\theta \in \left[-10^o, 10^o\right]$, parameters for Formula (7) $a = 0.1$, $b = 0.5$, and the replanting parameter for particles is $N_p = 16$. The selected simulation comparison algorithms are the standard LS algorithm and LPRLS algorithm proposed in the Thesis. The simulation results are shown in Fig.(a) to Fig.(e); the LPRLS algorithm is realized through studying toolbox function of malab level set, combining the algorithm theory proposed in the Thesis and preparing interface

procedure. Except the above parameter setting, the parameter settings of other level sets are the same as the parameter settings of level set algorithm in toolbox. The simulation results for evaluation indicators such as segmentation precision, time consumption and variance of level set algorithm are shown in Table 1. The simulation result in Table 1 is the average value for evaluation indicators obtained after respectively independent operation of the above two algorithms for 20 times.

Fig.4(a)-(e) respectively show the segmentation effects of LS algorithm and LPRLS algorithm on five groups of images such as angiography CT, tumor CT, breast CT, brain CT and chest CT. In Fig.(a) of angiography CT image segmentation, the identification rate of LPRLS algorithm in main vessels is evidently higher than that of LS algorithm, but the problem is that due to extremely high sensitivity, there are certain noise points for identification such as the small circles scattered in the figure; in Fig.(b) of tumor CT image segmentation, the segmentation by LPRLS algorithm for tumor contour is more comprehensive than that by LS algorithm and the more precise contour in tumor can be identified; in Fig.(c) of breast CT image segmentation, the identification by LPRLS algorithm for the whole breast is evidently more comprehensive than that by LS algorithm and the inner part of breast can also be segmented and identified in more precise way; in Fig.(d) of brain CT image segmentation, the structure of brain CT image is more complicated and the segmentation effect of LS algorithm is not satisfactory and its precision in segmentation is evidently lower than that of LPRLS algorithm; in Fig.(e) of chest CT image segmentation, the identification of LS algorithm in middle part of left chest is cluttered and the whole contour is also relatively cluttered, but the identification of chest contour by LPRLS algorithm is more comprehensive with better identification effect. Fig.2 shows the comparison of standard LS algorithm and LPRLS algorithm from the intuitive visual effect, so intuitively the LPRLS algorithm is evidently superior to the standard LS algorithm.

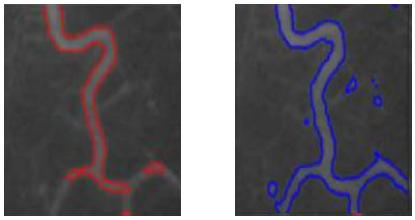


(a) Angiography CT Image

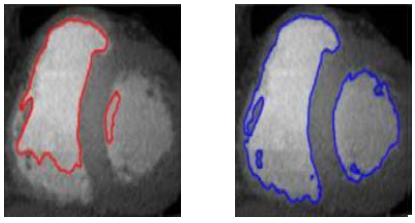


(b) Tumor CT Image

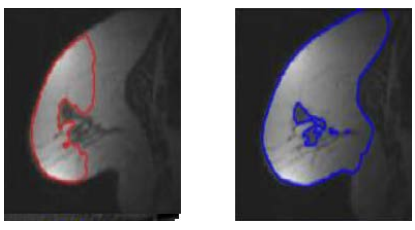

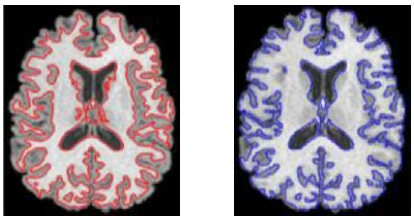

LS LPRLS

(d) Brain CT Image

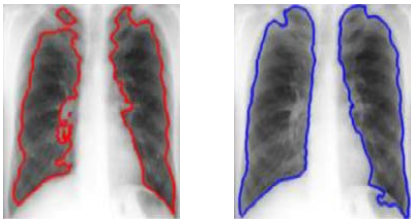

LS LPRLS

(e) Chest CT Image

Fig.2 LPRLS Level Set Segmentation

Table 1 respectively shows the comparison results of segmentation values for standard LS algorithm and LPRLS algorithm in five groups of images of angiography CT, tumor CT, breast CT, brain CT and chest CT. The simulation comparison indicators include identification rate, operation time and variance of identification rate and there are respectively 20 times to solve the average value for the algorithm. In segmentation identification rate indicators by the algorithms, LPRLS algorithm is evidently higher than the standard LS algorithm and the advantage is evident; in the indicator, the LPRLS algorithm is averagely 20%-30% higher, such as in three groups of images such as angiography CT, tumor CT and breast CT; the identification rate of standard LS algorithm is near 50%-60%, while the segmentation identification rate of LPRLS algorithm in the three groups of images reaches above 85%; in two groups of image segmentation for brain CT and chest CT, the standard LS algorithm slightly reaches above 70%, but the segmentation identification rate of LPRLS algorithm in the two groups of images reaches above 90%. In comparison of the calculated time indicators, the operation times for standard LS algorithm in the five groups of images are between 20s-35s, while the segmentation times of LPRLS algorithm in the five groups of images are distributed between 16s-20s, so it can be inferred that in calculation time, LPRLS algorithm is also superior to the standard LS algorithm. In the algorithm variance indicators representing the stability of algorithm, LPRLS algorithm is slightly superior to the standard LS algorithm with little difference.

Table 1 Operation Indicators of Algorithms

| Algorithm | Image type | Identification rate | Operation time | Variance |
|---|---|---|---|---|
| LS Standard LS | Angiography CT | 68.15% | 25.63s | 5.32% |
| | Tumor CT | 52.31% | 20.27s | 7.19% |
| | Breast CT | 62.37% | 21.35s | 6.83% |
| | Brain CT | 73.56% | 33.68s | 6.93% |
| | Chest CT | 82.64% | 20.89s | 8.24% |
| LPRLS | Angiography CT | 88.64% | 19.63s | 4.61% |
| | Tumor CT | 95.34% | 18.19s | 4.18% |
| | Breast CT | 85.49% | 17.53s | 4.93% |
| | Brain CT | 91.59% | 19.57s | 6.38% |
| | Chest CT | 92.64% | 16.62s | 5.12% |

## Conclusion

With regard to the relatively significant influence of uneven pixel of medical CT image on local segmentation algorithm for image, the medical CT image segmentation algorithm of hybrid level set based on Lagrangian particle enhanced replanting algorithm is proposed. First, for the unevenness of local image, calculate the Lagrangian labeled particle before calculating the formula of horizontal set to rebuild the embedded interface in order to improve the mass conservation property of level set algorithm; secondly, for the uncertainties of traditional particle method in processing interface singularity and complicated geometric correlation problem, improve the convergence of velocity field for singular point and topological change point through increasing velocity vector and unit normal vector; finally, the test set of synthetic data and simulation test of real CT image indicate that the proposed algorithm is superior to the comparison algorithm in edge segmentation convergence precision and operation speed.

## Acknowledgement

Supported by Fundamental and Advanced Technology Research Project of Henan, China ( No. 162300410188),Supported by Fundamental and Advanced Technology Research Project of Henan, China ( No. 162300410269)

## Reference

[1] Yang X, Zhao W, Chen Y, et al. Image segmentation with a fuzzy clustering algorithm based on Ant-Tree[J]. Signal Processing, 2008, 88(10):2453-2462.

[2] Huang C, Yan B, Jiang H, et al. MR Image Segmentation Based On Fuzzy C-Means Clustering and the Level Set Method[C]// International Conference on Fuzzy Systems and Knowledge Discovery. IEEE, 2008:67-71.

[3] Yu J, Wang Y. Molecular image segmentation based on improved fuzzy clustering[J]. Journal of Biomedical Imaging, 2007, 2007(1):4-4.

[4] Bai P R, Liu Q Y, Li L, et al. A novel region-based level set method initialized with mean shift clustering for automated medical image segmentation[J]. Computers in Biology & Medicine, 2013, 43(11):1827-1832.

[5] Li K, Guo Z. Image Segmentation with Fuzzy Clustering Based on Generalized Entropy[J]. Journal of Computers, 2014, 9(7).